

Ion source antenna development for the Spallation Neutron Source

R. F. Welton,^{a)} M. P. Stockli, and Y. Kang

Accelerator Systems Division, Spallation Neutron Source, Oak Ridge National Laboratory, Oak Ridge, Tennessee 37830-6473

M. Janney

Metals and Ceramics Division, Oak Ridge National Laboratory, Oak Ridge, Tennessee 37830-6087

R. Keller, R. W. Thomae, and T. Schenkel

Lawrence Berkeley National Laboratory, Berkeley, California 94720

S. Shukla

University of Tennessee, Knoxville, Tennessee 37916

(Presented on 6 September 2001)

The operational lifetime of a radio-frequency (rf) ion source is generally governed by the length of time the insulating structure protecting the antenna survives during exposure to the plasma. Coating the antenna with a thin layer of insulating material is a common means of extending the life of such antennas. When low-power/low-duty factor rf excitation is employed, antenna lifetimes of several hundred hours are typical. When high-power, >30 kW, and high-duty cycles, ~6%, are employed, as is the case of the Spallation Neutron Source (SNS) ion source, antenna lifetime becomes unacceptably short. This work addresses this problem by first showing the results of microanalysis of failed antennas from the SNS ion source, developing a model of the damage mechanism based on plasma-insulator interaction, using the model to determine the dimensional and material properties of an ideal coating, and describing several approaches currently under way to develop a long-lived antenna for the SNS accelerator. These approaches include thermal spray coatings, optimized porcelain enamel coatings, refractory enamel coatings, and novel antenna geometries designed to operate with low rf electric fields. © 2002 American Institute of Physics.

[DOI: 10.1063/1.1431416]

I. INTRODUCTION

The ion source for the Spallation Neutron Source (SNS) is currently under construction at Lawrence Berkeley National Laboratory (LBNL). The source is a rf, multi-cusp, volume-type H^- ion source that employs a helical rf antenna consisting of a copper conductor encased in an insulating porcelain enamel coating 100–200 μm in thickness. The source is required to deliver 35–50 mA of H^- within a 1 ms macropulse at a repetition rate of 60 Hz over an operational lifetime of ~500 h.¹ This current requirement necessitates the use of high rf powers, 30–50 kW, which, when applied over the duty cycle of 6%, results in a high likelihood of antenna failure within several hours of operation.

Traditionally, little attention has been paid to the detail of the antenna coating and the coating processing since acceptable antenna lifetimes were easily achieved under modest source operating conditions. Given the more stringent requirements of the SNS and other high power accelerators currently under development, the need to increase our understanding of the antenna failure mechanism and conceive of solutions is clear. For several years, P&G Corporation² has been manufacturing and distributing porcelain-coated antennas to several accelerator facilities worldwide. Other antenna protection schemes have been developed³ which include a

helical quartz tube enclosing a stainless steel or Ti water-cooled antenna,⁴ and a cylindrical Al_2O_3 liner between the antenna and plasma.⁵ After considerable experimentation at LBNL, we have been unable to produce the required H^- current with the quartz enclosed antenna and have therefore focused our effort on improved porcelain and ceramic coatings. On the other hand, DESY has had considerable success producing ~40 mA of H^- for 7000 h at 0.05% duty factor (60 h equivalent time at 6% duty factor) using an Al_2O_3 liner.⁵

II. ANTENNA FAILURE MECHANISM

We have examined a number of P&G antennas that have failed in service during tests at LBNL. After the antennas have been run for several hours, 1–4 visible localized damaged areas or “hot spots,” can be observed on the porcelain coating and are oriented in apparently random directions. If the damaged area penetrates the entire thickness of the coating the source no longer produces high-density plasma and the antenna must be replaced. Figure 1 shows a microscopic image, with a magnification of 200 \times , of a cross-sectional view cut through the antenna at a typical damaged region. The sample was prepared using standard metallographic techniques of cutting and polishing. Evident in the figure are the presence of numerous pores throughout the porcelain enamel coating. A considerable increase in the size of the pores near the center of the damaged region is also evident. Examination of undamaged regions shows much smaller-

^{a)}Electronic mail: welton@sns.gov

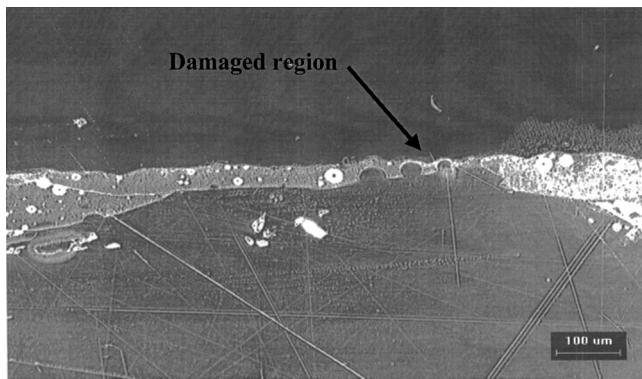


FIG. 1. Micrograph (magnification: 200 \times) of a cross section of a P&G-coated antenna cut through a typical damaged region shown near the center of the figure.

pore size, suggesting that localized temperatures in the damaged area exceeded the melting point of the enamel composition, $\sim 800^\circ\text{C}$, causing the pores to coalesce and grow in size. Also, most porcelain enamels and glasses become electrically conductive in the liquid state. Approximately 10% by volume of TiO_2 was also observed in the enamel composition, a common practice employed to give the enamel an opaque appearance.

The SNS ion source antenna operates with rf voltages of ~ 1 kV under normal operating conditions. This potential can be determined from measured antenna currents of ~ 200 A and the inductance of the antenna ~ 0.5 μH . Since one leg of the antenna is tied to the plasma chamber, this ~ 1 kV must appear across the antenna coating insulator and across the plasma sheath adjacent to the ungrounded leg. A reasonable picture of the failure process can be painted as follows: a defect or thin place in the coating or a defect in antenna conductor creates a region of locally enhanced electric field. Positive ions from the plasma will be accelerated into the antenna surface during the negative cycle of the rf wave with sufficient energy to eject surface atoms (sputtering) and surface electrons (secondary electron emission) if a sufficient plasma sheath potential is present. This process, being driven by strong capacitive coupling between the rf field and the plasma, and being aided by a flux of ejected particles from the “active” spot on the antenna surface, can substantially heat the surface and produce penetrations in the antenna coating. The critical step in this picture is that the voltage drop across the rf plasma sheath must be sufficient to initiate and drive the destruction of the coating. If the electrical properties of the coating were chosen so that most of the potential difference between the plasma and antenna conductor would appear across the coating rather than the plasma sheath, the likelihood of this type of antenna failure would be greatly reduced if not eliminated.

This approach is embraced by the fusion energy community where coatings employed for the protection of plasma facing antennas used in ion cyclotron resonance frequency (ICRF) heating of fusion devices are designed so that sheath voltages are kept as low as possible.⁶ In fact, the formation of hot spots and arcs on antenna surfaces in ICRF systems has been directly attributed to high sheath voltages.⁷ We will show in the following section that the very thin antenna coat-

ings used in the current P&G antennas (~ 200 μm) only partially reduce the sheath potential, offering the coating little protection from plasma bombardment.

III. SHEATH-INSULATOR MODEL

Here we determine the thickness, dielectric constant, electrical resistivity, and dielectric breakdown strength of the antenna coating, which are required to reduce sheath potentials to acceptable values. The approach taken in Ref. 6 is followed very closely with the exception that plasma parameters of the SNS ion source are used rather than those associated with the fusion plasma. If ΔV represents the instantaneous voltage difference between the plasma and antenna conductor and V_s and V_i represent the voltage across the sheath and insulating coating, respectively, we can write

$$\frac{V_s}{\Delta V} = \frac{V_s}{V_s + V_i} = \frac{Z_s}{Z_s + Z_i}. \quad (1)$$

Here Z is the impedance of the sheath or insulating coating, specified by the subscript, which is calculated considering the capacitive component of the impedance and resistance to be summed as a parallel circuit, $Z^{-1} = X^{-1} + R^{-1}$, following Ref. 6.

Consider first, the impedance across the insulating coating. The resistive component of the impedance across the coating is

$$R_i = \eta \frac{d}{A}, \quad (2)$$

where d is the coating thickness, η is coating materials resistivity, and A is a unit area. The capacitive component of the impedance across the coating can be estimated by

$$X_i = \frac{1}{\omega C} = \frac{d}{\epsilon_0 K \omega A}, \quad (3)$$

where K is the coating materials dielectric constant, $\omega = 2\pi f$ is the rf angular frequency, and ϵ_0 is the permittivity constant.

To estimate the impedance across the sheath, the sheath thickness Δ must first be determined and the customary approximation of a collisionless, Child–Langmuir sheath is employed³

$$\Delta = \lambda_D \left(\frac{e V_s}{k T_e} \right)^{3/4}, \quad \lambda_D = \left(\frac{\epsilon_0 k T_e}{n_e e^2} \right)^{1/2}, \quad (4)$$

where n_e and T_e are the plasma density and temperature, respectively. The electron density and temperature have been measured in a source very similar to SNS source and found to be 6 eV and $\sim 10^{12}$ cm^{-3} , which have been held constant for these calculations.⁸ The capacitive component of the impedance across the sheath is then given by

$$X_s = \frac{\Delta}{\epsilon_0 \omega A}. \quad (5)$$

Again, following the analysis in Ref. 6, the resistive component of the impedance across the sheath can be determined from power dissipation arguments to be

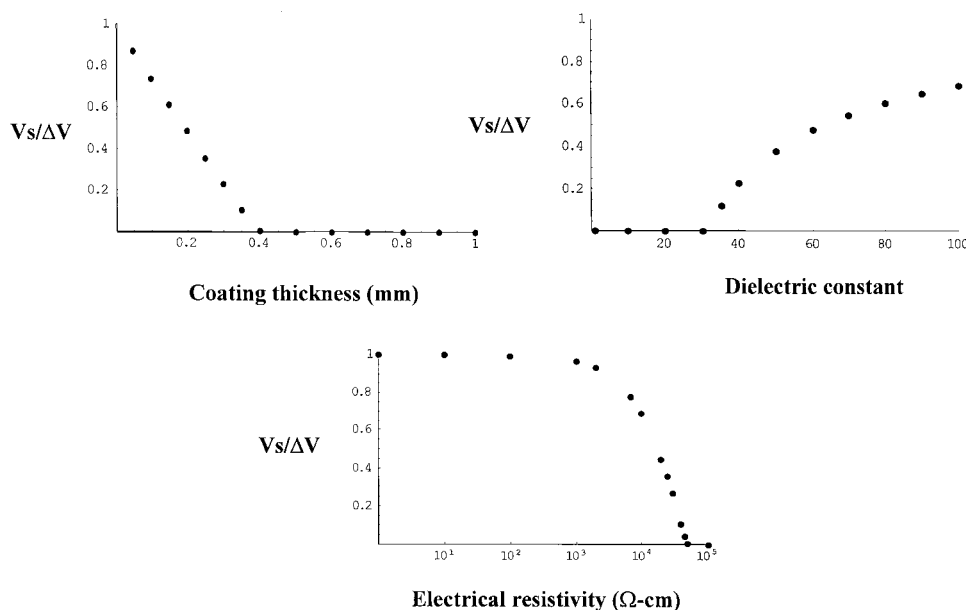


FIG. 2. Numerical computation of the fractional voltage across the plasma sheath vs the dielectric constant K , electrical resistivity η , and thickness d of the insulating antenna coating. All parameters were fixed at $n_e = 10^{12} \text{ cm}^{-3}$, $T_e = 6 \text{ eV}$, $K = 12$, $\eta = 10^{14} \Omega \text{ cm}$, $d = 1 \text{ mm}$ unless varied in the plot.

$$R_s = \frac{V_s m I_0(eV_s/kT_e)}{2eA n_e k T_e I_1(eV_s/kT_e)}, \quad (6)$$

where I_0 and I_1 are Bessel functions and the other symbols have their usual values.

By substituting Eqs. (2)–(6) into Eq. (1), a nonlinear equation in V_s can be obtained, allowing $V_s/\Delta V$ to be determined uniquely for a given set of parameters: n_e , T_e , K , η , and d . Since this equation cannot be solved explicitly for V_s , a numerical algorithm has been employed to calculate $V_s/\Delta V$. Figure 2 shows plots of $V_s/\Delta V$ vs K , η , and d , holding the other parameters fixed at nominal values of $n_e = 10^{12} \text{ cm}^{-3}$, $T_e = 6 \text{ eV}$, $K = 12$, $\eta = 10^{14} \Omega \text{ cm}$, and $d = 1 \text{ mm}$, which are typical of porcelain enamel compositions.⁹ The figure shows that in order to effectively reduce the sheath potential below the sputtering threshold for H on SiO_2 ¹⁰ (approximate for porcelain) and below secondary electron multiplication on the surface,¹¹ energies less than $\sim 30 \text{ eV}$ are required. Figure 2 shows that a coating thickness of $\sim 400 \mu\text{m}$ is required to reduce the sheath potential to these values. Note this value is twice as large as the nominal P&G antenna coating thickness. If we consider lower plasma densities, such as those which might occur between the turns of the antenna or between the antenna and plasma chamber, even larger values of d are required to reduce the sheath potential. Thus we choose to consider the conservative dimension of $d = 1 \text{ mm}$ for these studies. The figure also shows that for 1-mm-thick coatings, the dielectric constant of the coating must be less than $K = 30$ in order to fully reduce the sheath potential. Figure 2 also shows that the electrical resistivity of the coating needs to be greater than $45\,000 \Omega \text{ cm}$ in order to fully mitigate the sheath potential. Note: since most porcelain enamels ideally have a resistivity of $\eta \sim 10^{14} \Omega \text{ cm}$, this condition is easily satisfied.

This design philosophy of carrying essentially the entire rf voltage across the insulator coating places emphasis on another material and structural property of the antenna coating: dielectric breakdown strength. For this example, the dielectric strength of the as-prepared coating must be in excess

of $\sim 1 \text{ kV/mm}$. Fortunately, this value is well below the dielectric strength of many high-quality porcelain coatings that tend to be on the order of 10 kV/mm .⁹ In practice, structural defects can reduce this value considerably and we, therefore, must test (high-pot) antennas submerged in salt water to ensure that the coating can hold voltages in excess of $\sim 1 \text{ kV/mm}$.

If, as we have shown from an electrical point of view, thicker coatings are desirable, what are the thermal consequences of such a change? The temperature gradient across the coating can be calculated in the normal operating mode of the SNS ion source, not the atypical mode associated with localized damage to the antenna. At 6% duty cycle, the average heat load on the plasma facing portion of the antenna can be calculated to be $q \sim 5 \text{ W/cm}^2$. In one dimension, simple conduction theory states that the temperature gradient across the coating is $\Delta T = qd/k$, where k is the thermal conductivity of the porcelain or $\sim 1 \text{ W/mK}$.⁹ We see that a temperature gradient of only 50°C develops across a $d = 1 \text{ mm}$ coating. The thermal stress induced by this temperature gradient can easily be handled by most porcelains.⁹ Damage to the coating as a result of direct heating by the rf field is less problematic since the heating is approximately uniform through the thickness and can be shown to be only $\sim 5 \text{ W/cm}$ of antenna length. Heat loads from the antenna conductor can be ignored since it is directly water cooled.

Thus, this electrical analysis has shown the need to develop antennas with thicker, low dielectric constant, high electrical breakdown strength (low porosity) coatings and that the current generation of P&G coatings is not meeting these conditions. Sections IV–VI detail our efforts to develop coatings with these qualities.

IV. OPTIMIZED PORCELAIN COATINGS

We have begun a close collaboration with a local porcelain enamel house, Cherokee Porcelain Corporation (CP)¹² to develop antenna coatings with a higher degree of uniformity, lower porosity, greater thickness, and lower dielectric con-

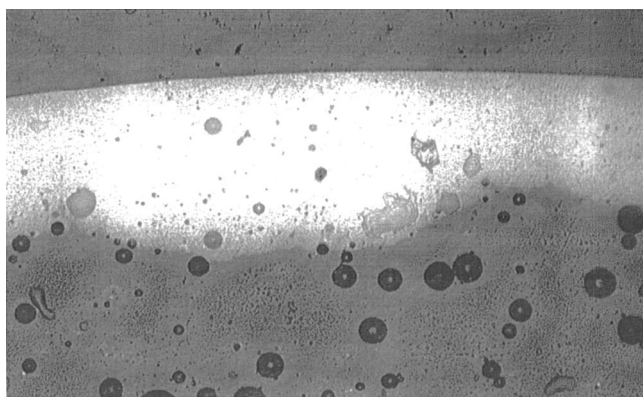


FIG. 3. Micrograph (magnification: 200 \times) of a cross section of the bilayer coating developed by Cherokee Porcelain Corp. The cover coat (top) shows a very low degree of porosity while the base coat (bottom) shows considerable porosity.

stant compared with the nominal P&G antenna. Figure 3 shows an example cross-sectional micrograph of a bilayer CP coating. The base coat composition has been optimized for mechanical adhesion to the copper, and the porosity in the base coat is intentionally added to reduce the shear strain, which results from the large difference in thermal expansion coefficient between copper and porcelain. The cover coat composition has been optimized for high dielectric breakdown strength with a coating density of nearly 100%. To date, uniform coatings have been deposited with a thickness of $\sim 1000\ \mu\text{m}$ (1 mm) using ~ 10 porcelain spray coat/firing steps. Antennas prepared in this manner have withstood potentials of 3 kV applied across the coating, which is the limit of our power supply used in the saltwater test rig. The dielectric constant of the coating has also been reduced substantially by removal of the TiO_2 component in the porcelain compared with the P&G antennas. An initial test of a CP antenna with a coating of only $300\ \mu\text{m}$ of porcelain was performed at LBNL; the antenna was run in an ion source at 6% duty cycle, for over ~ 100 h at 25 kW of rf power without failure. This initial test suggests a significant lifetime improvement over the P&G antennas, although statistics are needed to verify this. In spite of these good results, faint cracks are visible in the enamel surface and subsurface and may be problematic: they are formed in manufacture and likely result from the large mismatch in the coefficient of

thermal expansion between copper and porcelain. Efforts to reduce or eliminate crack formation are currently being pursued (see Sec. VI).

V. THERMAL SPRAY COATINGS

Thermal spray technologies, which include plasma spray and the newly developed high-velocity-oxy-fuel (HVOF) spray techniques, offer the possibility of depositing very dense, arbitrarily thick coatings of highly refractory materials, such as Al_2O_3 , directly onto the antenna.¹³ Coatings with a density of 99.5% have been successfully applied to planar copper surfaces and are used for a wide variety of applications.¹⁴ Several attempts were made by TST Coatings Corporation¹⁴ to coat the rather complex geometry of the helical antenna: plasma spray of Cr_2O_3 and HVOF spray of Al_2O_3 on copper antenna bodies. Although, the coatings appeared visually to be of high quality, they failed saltwater high-pot tests, indicating the presence of substantial open porosity. They also failed immediately when tested in the ion source, and we have abandoned this approach.

VI. REFRACTORY ENAMEL COATINGS

One of the largest hurdles encountered in the present porcelain-copper system is the large thermal expansion mismatch between the metal and the glass coating, which generates large thermal stresses during manufacture, resulting in the formation of shallow cracks. A potential replacement is based on a coil of niobium or tantalum coated with a refractory seal glass composition consisting of Al_2O_3 , CaO , and MgO .¹⁵ This materials system is used widely in the manufacture of high intensity discharge lamps and ceramic metal halide lamps. The thermal expansion mismatch in this system is about $1 \times 10^{-6}\ \text{cm/cm/}^\circ\text{C}$, as compared with a difference of about 8×10^{-6} for the copper-enamel system. This greatly reduces the stresses introduced during manufacture. In addition, the seal glass systems are composed of much more refractory materials than the porcelain enamels. Typical seal glasses melt in the range of 1400°C , as compared with 800°C for the enamels. At Oak Ridge National Laboratory, we have begun coating experiments on this system.

VII. TRANSVERSE ANTENNA DESIGN

Another approach to reducing the likelihood of antenna coating failure is to reduce the peak rf electric field associ-

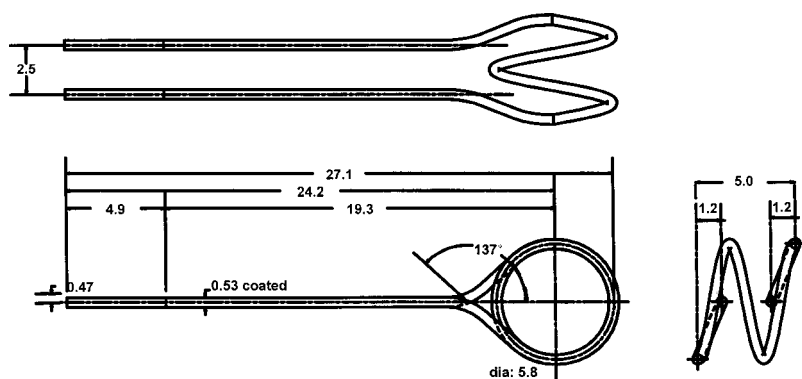


FIG. 4. Mechanical drawing of the transverse antenna designed to operate with low peak rf electric fields. All dimensions are in cm.

ated with the antenna by altering the antenna geometry in addition to changing the antenna coating properties. The three-dimensional software, High Frequency Structure Simulator¹⁶ has been used to help design a new antenna shape that operates with a low nominal rf electric field. The resulting design is shown in Fig. 4 and had the lowest field of the various cases investigated: 2.2 kV/cm without a plasma approximation and 0.56 kV/cm with a plasma approximation were included in the simulation. These numbers should be compared with simulation of the standard antenna geometry, which yielded values of 5.2 kV/cm without a plasma approximation and 1.6 kV/cm with a plasma approximation. Thus, the new design should operate with a peak E-field strength a factor of ~ 2 – 3 lower than the standard antenna. We plan to test this antenna design in an ion source shortly.

ACKNOWLEDGMENT

The SNS is managed by UT-Battelle, LLC, under Contract No. DE-AC05-00OR22725 for the U.S. Department of Energy.

- ¹R. Keller *et al.*, Rev. Sci. Instrum. (these proceedings).
- ²Porcelain Patch and Glaze Corporation, Oakland, CA.
- ³M. A. Lieberman, *Principles of Plasma Discharges and Materials Processing* (Wiley-Interscience, New York, 1994).
- ⁴J. Reijonen *et al.*, Rev. Sci. Instrum. **71**, 1134 (2000).
- ⁵J. Peters, Rev. Sci. Instrum. **71**, 1069 (2000).
- ⁶J. R. Myra *et al.*, J. Nucl. Mater. **249**, 190 (1997).
- ⁷M. Bures, Nucl. Fusion **32**, 1139 (1992).
- ⁸D. S. McDonald, Rev. Sci. Instrum. **63**, 2741 (1992).
- ⁹A. I. Andrews, *Porcelain Enamels*, 2nd ed. (Garrad, Champaign, IL, 1961).
- ¹⁰W. Eckstein, C. Garcia-Rosales, J. Roth, and W. Ottenberger, Technical Report No. IPP9/82, Sputtering Data, Max-Planck-Institut Fur Plasma-physik, 1993.
- ¹¹G. F. Dionne, J. Appl. Phys. **46**, 3347 (1975).
- ¹²Cherokee Porcelain Enamel Corp., 2717 Independence Lane, Knoxville, TN 37914.
- ¹³S. Sampath and X. Jiang, Mater. Sci. Eng., A **304–306**, 144 (2001).
- ¹⁴TST Coatings Corp., 515 Progress Way, Sun Prairie, WI 53590.
- ¹⁵S. A. Mucklejohn and B. Preston, World Congress on Industrial Applications of Electrical Energy and 35th IEEE-IAS Annual Meeting, Rome, Italy, 2000, Vol. 5, p. 3326.
- ¹⁶Ansoft Corp., Four Station Square, Suite 200, Pittsburgh, PA 15219.